STATIC PRESSURE DISTRIBUTION IN A CHANNEL WITH OUTFLOW OF LIQUID THROUGH PERFORATED WALLS WITH A DENSE PATTERN OF NORMAL APERTURES

A. D. Rekin

UDC 532.545

The static pressure distribution along a channel is found using a one-dimensional equation based on the flow momentum equation. A comparison of results of experiments conducted and calculations with coefficients accounting for the two-dimensionality of the flow shows good agreement.

In the design of some types of engineering equipment, one meets the problem of the distribution of flow rate of liquid (or gas) along a channel with outflow through perforated side walls to the surrounding medium. The discharge law through normal apertures whose thickness is less than or close to the aperture diameter ($\Delta/d \leqslant 1$) can be represented, according to the Bernoulli law, in the following form:

$$v_w = \mu c \sqrt{2(p - p_a)/\rho}. \tag{1}$$

Here the discharge coefficient μ mainly describes the compression of the cross section of jets in apertures (the pressure losses due to viscosity of an actual liquid are usually small for thin walls). It follows from the theoretical solution of [1] that for discharge of an ideal liquid from a channel with thin walls the value of μ for a single aperture with $d/R \ll 1$ is uniquely determined by the parameter $(p - p_a)/q$. It was shown that for $(p - p_a)/q \to 0$ the value $\mu \to 0$, while for $(p-p_a)/q \gg 1$ it tends asymptotically to the limiting value μ_∞. From the results of experiments conducted with discharge of air through the perforated walls of a pipe with normal apertures $d/\Delta \approx 1$ and permeability $c \leqslant 0.05$, reference [2] proposed the relation

$$\mu = \mu_\infty [1 - \exp(-\sqrt{2(p - p_a)/q})], \tag{2}$$

which agrees with theory for a single aperture. Thus, the distribution of liquid flow rate along a channel with the indicated perforation of the walls is determined uniquely by the distribution of static pressure drop at the wall.

A one-dimensional description of flow in a channel with efflux of liquid through perforated walls has been given in great detail in [3, 4]. From the equation of motion averaged in terms of flow rate over the channel cross section one obtains an equation for the mean velocity. In solving this one assumes a constant value for the discharge coefficient along the channel, and the friction factor, according to the approximation of [5], based on reduction of results of tests in a pipe with porous walls and relatively small outflow velocity ($v_w/u_0 \leqslant 0.1\lambda_0$):

$$\lambda = \lambda_0 + 3{,}56 v_w/u. \tag{3}$$

The theoretical data agree well with the results of tests made with a perforated pipe with a uniform flow velocity profile at the pipe entrance. Agreement of results of theory and tests with a developed velocity profile at the pipe entrance was obtained by allowing for a coefficient averaging the square of the velocity according to the flow rate $\alpha > 1$.

In the present paper, as was done in [3, 4], a one-dimensional description is given of the integral flow characteristics along the channel. As the governing parameter we chose the static pressure (the tests of [4, 6] and our own tests indicate that the static pressure over the radius of a perforated or a porous pipe with outflow is practically constant; the error is a quantity on the order $\rho v_w^2/2p$). An equation describing the pressure distribution along a straight channel with constant area of cross section is obtained by integrating the equation of motion over the channel area under the assumption of axisymmetric flow

Translated from Inzhenerno-Fizicheskii Zhurnal, Vol. 45, No. 6, pp. 933-940, December, 1983. Original article submitted June 29, 1982.

 0022-0841/83/4506-1388$07.50

$$Fd\,(p+\beta\rho u^2)/dx = -(c_f\rho u^2/2 + \rho v_w u_w)\,z. \quad (4)$$

We shall first analyze the right side of Eq. (4). As a rule, for porous walls one assumes the condition of liquid attachment at the wall ($u_w = 0$). Evidently this condition can be assumed, approximately, also for perforated walls for which $d/\Delta \leqslant 1$. A direct confirmation of the validity of this condition comes from the results of tests conducted with water flow in a perforated pipe: the water jets discharge from apertures of the pipe with $d/\Delta \leqslant 2$ practically perpendicular to the walls if there is no auxiliary flow on the outside. For $d/\Delta > 2$ the water jets at the outlet have a longitudinal velocity component. In this case one must introduce a slip parameter $u_w/u > 0$.

Reference [7] has determined experimentally the dependence of λ (for a pipe $\lambda = 4c_f$) on liquid outflow intensity for turbulent flow in a perforated pipe with normal apertures in the wall. In the experiments the internal diameter of the thick-walled pipe was 20 mm, the diameter of the apertures was 2 mm, and the pitch between apertures was s = 4.8-25 mm. Along the pipe axis there was a tube of diameter 6 mm, used to measure the static pressure. Reduction of the experimental data with $s \leqslant 8$ and $v_w/u = (0\text{–}2.5)\lambda_0$ gives the recommended formula $\lambda = \lambda_0 + 15.6(v_w/u)^{1.27}$.

Values of λ for s = 25 mm proved to be larger than for $s \leqslant 8$ mm, and were therefore not included in the proposed correlation. The results of the tests of [7] with $s \leqslant 8$ mm were reduced in [8] using the outflow parameter b. In this reduction the parameters were approximated with satisfactory accuracy by the formulas [9]

$$\lambda = \lambda_0 (1 + b/4)^2,\ b \leqslant 4;\ \lambda = 8v_w/u,\ b \geqslant 4, \quad (5)$$

which were derived and verified experimentally for turbulent flow over a porous flat plate with boundary layer suction.

The results of the tests for perforated walls can be approximated by these formulas, evidently, only for $d/\Delta \leqslant 2$ and a dense arrangement of apertures, as was achieved in [7] with $s \leqslant 8$ mm.

In order to simplify Eq. (4) we shall represent the dependence $\lambda(b)$ in a different way than Eq. (5). By comparing the integral momentum equations for a boundary layer on a flat plate [9] with and without suction we obtain

$$c_f = c_{f_0}\psi + 2v_w/u_\infty,$$

where $\psi = (d\vartheta/dx)/(d\vartheta_0/dx)$; ϑ is the momentum loss thickness; and u_∞ is the velocity outside the boundary layer. As applied to a pipe (porous or perforated with $d/\Delta \leqslant 2$) we write this formula in the form

$$\lambda = \lambda_0\psi + 8v_w/u. \quad (6)$$

Here the quantity ψ describes the relative fraction of the friction factor not associated directly with outflow of liquid, and can be expressed by any relation giving a good approximation to the experimental data. A comparatively simple form is the relation

$$\psi(b) = \exp(-b/2 - b^2/4). \quad (7)$$

The results of calculating λ/λ_0 from Eqs. (6) and (7) give a good description of the experimental data of [7] for $s \leqslant 8$ mm, and practically coincide with values from Eq. (5) for all values of b, and from Eq. (3) in the range $b \leqslant 1$ for which this formula was obtained. We note an important conclusion following from Eqs. (5) and (6) with intense outflow ($b \geqslant 4$, $\psi \to 0$): the tangential friction stress on a porous wall is independent of the liquid viscosity and is determined only by the outflow velocity $\tau_w = \rho v_w u$. This resistance of the wall is called the discharge resistance [10]. In the case of a nonuniform longitudinal vlocity profile across the channel section it will be expressed by the relation $\tau_w = \rho v_w u_m$, where u_m is the longitudinal velocity of jets discharging from the channel, in the main flow prior to discharge. Therefore, in this case the friction factor can be represented in the form

$$\lambda = \lambda_0\psi(b) + 8\varepsilon v_w/u, \quad (8)$$

where $b = \rho v_w u_m/\tau_{w_0}$; $\varepsilon = u_m/u$.

Substituting Eq. (8) into Eq. (4), for the condition $u_w = 0$ ($d/\Delta \leqslant 2$) we obtain the following expression for change of the total flow momentum:

$$Fd\,(p+\beta\rho u^2)/dx = -(\lambda_0\psi\rho u^2/8 + \varepsilon\rho v_w u)\,z. \quad (9)$$

TABLE 1. Characteristics of the Perforated Pipes

Pipe number	d, mm	s, mm	c
1	0,8	5	0,0227
2	0,8	10	0,0113
3	1,2	10	0,0255
4	1,7	10	0,0510
5	2,0	20	0,0233

Hence it follows that for $b \geqslant 4$ and a dense arrangement of apertures ($\psi \to 0$) the total flow momentum is reduced in the same way as for an ideal liquid, only by the loss of momentum of the discharging liquid which has velocity u_m prior to discharge. For a uniform distribution of longitudinal velocity in the pipe ($\beta = \varepsilon = 1$) from Eq. (9) we obtain an equation for the change in the total pressure ($p^* = p + \rho u^2/2$):

$$\frac{dp^*}{dx} = -\frac{\lambda_0 \psi}{2R} \rho \frac{u^2}{2}, \tag{10}$$

i.e., for $b \geqslant 4$ ($\psi \to 0$) the total pressure does not change along the channel (all of the boundary layer is sucked away through the wall).

Substituting Eq. (1) for v_w and the liquid continuity condition $F(du/dx) = -zv_w$ into Eq. (9) we obtain

$$\frac{dP}{d\bar{x}} = -\left(\frac{\lambda_0}{2}\psi + 2\frac{d\beta}{d\bar{x}}\right)\bar{u}^2 + 4(2\beta - \varepsilon)\mu c\sqrt{P}\,\bar{u} + \frac{1}{q_0}\frac{dp_a}{d\bar{x}}, \tag{11}$$

where $P = (p - p_a)/q_0$; $\bar{u} = 1 - 2\int_0^{\bar{x}} \mu c\sqrt{P}\,d\bar{x}$; $\mu(\sqrt{P}/\bar{u})$ is determined by Eq. (2); and the function $p_a(\bar{x})$ is considered as given. The two-dimensionality of the flow is accounted for by means of the coefficients β and ε.

In general Eq. (11) can only be solved numerically. An analytical solution is possible only when $2v_w/u \geqslant \lambda_0$ ($b \geqslant 4$) and β = const, ε = const over the whole length of the pipe. From this solution for p_a = const and $u_l = 0$ (closed end) it follows that

$$(p_l - p_0)/q_0 = 2\beta - \varepsilon, \tag{12}$$

i.e., only for $2\beta - \varepsilon = 1$, for example, for the condition of uniform flow ($\beta = \varepsilon = 1$) does the static pressure at the end of the pipe become equal to the total pressure at the entrance section.

In order to have some idea of the values of the coefficients β and ε which describe the two-dimensionality of the flow, we conducted tests with perforated pipes of internal diameter 20 mm and wall thickness 1 mm. In the perforated sections of the pipes of length l = 395 mm the normal apertures were arranged in a checkerboard pattern. The characteristics of the perforations are given in Table 1.

A turbulent stream of air with temperature equal to that of the surrounding medium (Re = $(5-20)\cdot 10^4$, T = 292-295°K) was supplied to the entrance of the pipe. The air discharged to the atmosphere through the perforated walls. At the pipe exit there was a valve to regulate the final air flow rate. In the tests we measured the air flow rate before and after the section investigated by means of specially calibrated orifice plates. We determined the static pressure distribution along the sections (the static pressure sensors were mounted at the wall; a determination of the static pressure in the flow showed that its variation over a single cross section of the pipe fell within the measurement accuracy). The pressures were measured by means of water piezometric tubes. The longitudinal velocity profiles were determined at several pipe sections by means of L-shaped tubes of external diameter 0.8 mm. Two types of profile were set up at the entrance: developed and practically uniform (with a thin boundary layer at the wall). The first profile was achieved using a precursor section of pipe of length 1 m, and the second was achieved by means of a grid mounted at a distance of 50 mm ahead of the perforated section (the wire diameter was 0.22 mm, the side length of the open square cell was 0.43 mm).

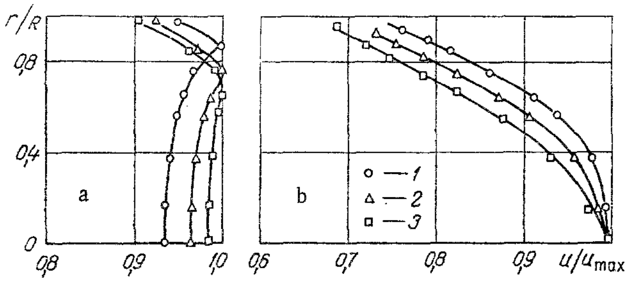

Fig. 1. Longitudinal velocity distribution at different cross sections of perforated pipe No. 3: a) with an equilibrating grid; b) with no grid: q_0 = 8.9 kPa; $\bar{u}_l = 0$; 1) x/R = 0; 2) 14; 3) 28.

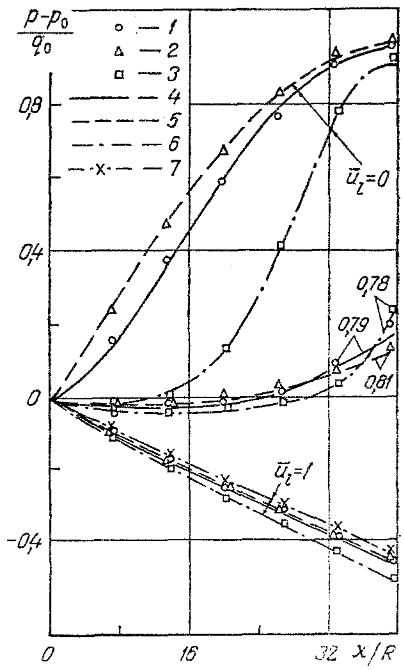

Fig. 2

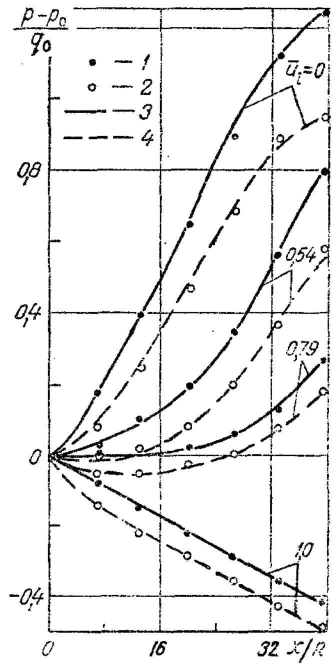

Fig. 3

Fig. 2. Static pressure distribution along perforated pipes with an initial uniform velocity profile: 1-3, 4-6) results of tests and calculations, respectively, for pipes Nos. 1, 2, and 4; 7) results of tests with a continuous permeable pipe; for pipe No. 1 $(p_0 - p_a)/q_0$ = 0.56; 0.17 and 1.04, respectively in the order of increasing $\bar{u}_l$; for pipe No. 2 the values are 2.75, 0.27, and 1.02; for pipe No. 4 the values are 0.053, 0.053, and 1.07.

Fig. 3. Static pressure distribution along perforated pipe No. 3: 1, 3) results of tests and calculations, respectively, for the developed initial velocity profile, $(p_0 - p_a)/q_0$ = 0.22, 0.095, 0.08, and 0.99, respectively, in order of increasing $\bar{u}_l$; 2, 4) the same for the uniform velocity profile, $(p_0 - p_a)/q_0$ = 0.375, 0.19, 0.155, and 1.05, respectively.

Figure 1 shows velocity profiles at three sections of Pipe No. 3 (including the entrance section at x = 0) for $\bar{u}_l = 0$. It can be seen that the initial uniform velocity profile is maintained up to the end of the perforated section (this was also noted in the tests of [4]). The developed velocity profile created at the entrance also changed little along the pipe, but became more convex. This is due to the influence of the considerable positive pressure gradient in the pipe for $\bar{u}_l$ (see Figs. 2 and 3) in an analogous way to flow of a liquid at constant flow rate in a diffuser channel: in the latter case the nonuniformity of the velocity field is increased. At a low value of outflow of air through the wall ($\bar{u}_l \approx 0.8$) in the tests there was equilibration of the initial developed velocity profile along the channel (in this case the pressure gradient along the channel is insignificant). The same variations of velocity profile as a function of the outflow velocity were recorded in tests with a porous pipe [6].

From the measured results presented in Fig. 1 one can conclude that the coefficients β and ε remain practically unchanged along the pipe in these tests. If we represent the velocity distribution over the pipe radius in the form of a power law $u/u_{max} = (1 - r/R)^m$, we obtain

$$\beta = (m + 1)(m + 2)^2/(8m + 4). \tag{13}$$

As m varies from 0 to 0.5 the value of β increases from 1 to 1.17. In our tests, for the velocity profiles shown in Fig. 1a we have $\beta \approx 1$, and for the profiles of Fig. 1b we have $\beta = 1.02\text{–}1.04$. We note that, according to the Schwartz integral inequality, $\beta \geqslant 1$ for any velocity distribution across the channel section. Estimates of the value of ε will be made below.

Figure 2 shows the results of the static pressure measurements in pipes Nos. 1, 2 and 4 with the uniform initial velocity distribution. The measured values are referenced to the mean flow velocity head at section x = 0, calculated according to the air flow rate $q_0 = G_0^2/(2\rho_0 F^2)$. The parameter is the relative flow rate at the end of the section $\bar{u}_l$. Figure 2 also shows the results of a numerical solution of Eq. (11) for $\beta = \varepsilon = 1$ at the indicated test conditions (a rapid convergence of the computation is obtained when one calculates from the end of the pipe). For the first series of apertures Eq. (7) for $\varphi(b)$ was made complicated in order to allow for a smooth variation of the friction factor from $\lambda = \lambda_0$ (with no outflow) at x = 0 to an equilibrium value calculated from Eq. (7), through the six series of apertures:

$$\psi = \exp\{[1 - \exp(-x/3s)](-b/2 - b^2/4)\}. \tag{14}$$

The value of λ_0 was determined from the same test, from the slope of the relations approximating to $p(\bar{x})$ in Fig. 2 with $\bar{u}_l = 1$ (the latter condition was achieved in the tests by covering the perforated sections from the outside by air-permeable insulating tape). To compare with the results of tests with $\bar{u}_l = 1$ we determined the static pressure distribution in the smooth (unperforated) pipe, cut from the same length of solid-drawn pipe from which the perforated test pipes were made. The term "smooth surface" here is arbitrary, since in the test range of $Re = (5\text{–}20)\cdot 10^4$ the value of λ_0 proves to be practically constant and is 0.02, i.e., the internal surface of all the sections was roughened for the conditions of the tests. Also, it follows from comparison of all the test results with $\bar{u}_l = 1$ that the value of λ_0 for the perforated pipes proved to be considerably larger than for the "smooth continuous pipe. To a first approximation this increase need not be accounted for in the calculations.

As can be seen from Fig. 2, the calculations give a good description of the test data. For $\bar{u}_l = 0$, both according to the calculations and according to the test results we obtain practically full recovery of static pressure at the end of the sections, to the stagnation pressure of the initial flow.

Tests were conducted with a similar perforated pipe No. 5 and a pitch of s = 20 mm. The pressure data proved to be somewhat lower than for pipe No. 1 with the same permeability but with finer perforations. For instance, with the uniform velocity profile at the pipe entrance and for $\bar{u}_l = 0$ the value obtained for $(p_l - p_0)/q_0$ was 0.91. This decrease of the quantity $(p_l - p_0)/q_0$ agrees with the results of the tests in [7] with s = 25 mm. Thus, one can conclude that the applicability of Eqs. (5) or (6) and (7) for perforated pipes is limited by the condition $s \leqslant R$. With a very sparse arrangement of apertures in the channel the value of ψ in Eq. (6) should evidently be taken as 1.

Figure 3 shows analogous results of tests with pipe No. 3 for the two types of initial velocity profile (a and b, respectively, in Fig. 1). Figure 3 also shows results of calculations using Eq. (11). For the uniform initial velocity profile over the entire pipe length we took $\beta = \varepsilon = 1$, and for the developed velocity profile we took $\beta = 1.02$, and the value of ε was chosen from the condition of making the calculation agree with the experimental data. The most suitable value proved to be $\varepsilon = 0.8$, which corresponds to $u_m/u_{max} = 0.65$ for the developed velocity profile. This means that only the wall-layer jets exit outside of the perforated pipe. For the developed velocity profile the value $u_m/u_{max} = 0.65$ corresponds to a distance from the wall approximately equal to the radius of the apertures (see Fig. 1b). Analogous results were obtained also in the tests with the other perforated sections.

Tests were conducted with pipe No. 3 with an entrance longitudinal velocity profile set up with a "dip" in the center (achieved using a group of grids). Here the value of $(p_l - p_0)/q_0$ in the tests with $\bar{u}_l$ was considerably less than 1. Thus, the results of the tests with long pipes ($\bar{l} = 40$) and different initial velocity profiles show that with a considerable outflow of liquid the "perturbations" from the wall do not propagate to the central jets of the stream and do not discharge from the pipe. The longitudinal velocity profiles at different pipe sections are formed under the influence of the longitudinal pressure gradient and turbulent mixing of the nondischarging jets. This is the reason for the constancy of the total pressure in the flow with the uniform initial velocity profile (see Eq. (10), $b > 4$).

The results of the tests of [4] agree qualitatively with the results of our tests for both the uniform and the developed velocity profile at the entrance section. However, for the conditions of [4] the original data are not adequate for performing calculations according to Eq. (11).

NOTATION

p, static pressure in the flow; p_a, pressure of the ambient medium; u, mean flow velocity; $\bar{u} = u/u_0$, relative flow velocity; ρ, liquid density; $q = \rho u^2/2$, velocity head of the flow; z, F, the perimeter and the cross-sectional area of the pipe, respectively; R, hydraulic radius of the channel; r, current radius in the pipe; x, longitudinal coordinate; $\bar{x} = x/R$; d, diameter of the apertures; Δ, wall thickness; s, pitch between apertures along the channel; c, permeability of the wall (relative area of the apertures); $v_w = -(F/z)du/dx$, conditional mean velocity of outflow from the channel; $b = \rho v_w u/\tau_{w_0}$, outflow parameter; c_f, $\lambda = 4c_f$, friction factor for a flat plate and a pipe; μ, discharge coefficient; $\beta = \int u^2 dF/(u^2 F)$, momentum average coefficient; u_m, velocity of jets in the stream later discharging from the channel; $\varepsilon = u_m/u$. Subscripts: 0, conditions at the channel entrance section or conditions without outflow of liquid; l, conditions at the end section; w, conditions at the wall.

LITERATURE CITED

1. G. S. Shandorov, "Discharge from a channel into a fixed and a moving medium," Zh. Tekh. Fiz., 27, No. 1, 156 (1957).
2. A. D. Rekin, "Experimental determination of the coefficient of discharge from a channel through perforated walls," Inzh.-Fiz. Zh., 43, No. 1, 54 (1982).
3. S. P. Sergeev, V. V. Dil'man, and V. S. Genkin, "Flow distribution in channels with porous walls," Inzh.-Fiz. Zh., 27, No. 4, 588 (1974).
4. A. S. Nazarov, V. V. Dil'man, and S. P. Sergeev, "Flow distribution in perforated channels with a permeable end," Inzh.-Fiz. Zh., 41, No. 6, 1009 (1981).
5. G. B. Wallis, "Pressure gradients for air flowing along a porous tube with uniform extraction at the wall," Inst. Mech. Eng. Proc. 1965-66, 180, No. 1, 1, 27.
6. J. K. Aggarwall, M. A. Hollinworth, and Y. R. Mayhew, "Experimental friction factors for turbulent flow with suction in a porous tube," Int. J. Heat Mass Transfer, 15, No. 9, 1585 (1972).
7. I. S. Kochenov and O. Yu. Novosel'skii, "The hydraulic resistance of channels with a permeable wall," Inzh.-Fiz. Zh., 16, No. 3, 405 (1969).
8. I. G. Meerovich and L. I. Zaichik, "Hydraulic resistances for motion of a liquid in channels with permeable walls," Teplofiz. Vys. Temp., 14, No. 6, 1222 (1976).
9. S. S. Kutateladze and A. I. Leont'ev, Heat and Mass Transfer and Friction in the Turbulent Boundary Layer [in Russian], Énergiya, Moscow (1972).
10. H. and K. Schlichting, Boundary Layer Theory, McGraw-Hill (1968).